

Prior knowledge-guided multilevel graph neural network for tumor risk prediction and interpretation via multi-omics data integration

Hongxi Yan[†], Dawei Weng[†], Dongguo Li, Yu Gu, Wenji Ma and Qingjie Liu

Corresponding authors: Yu Gu, School of Biomedical Engineering, Capital Medical University, 10 You An Men Wai, Xi Tou Tiao, Beijing 100069, China.

Tel.: 18500087987, E-mail: ygu@ccmu.edu.cn; Wenji Ma, Center for Single-Cell Omics, School of Public Health, Shanghai Jiao Tong University School of Medicine, 227 South Chongqing Road, Shanghai 200025, China. Tel.: 18612370689, E-mail: wenjimacs@sjtu.edu.cn

[†]Hongxi Yan and Dawei Weng contributed equally to this work and also joint first authors.

Abstract

The interrelation and complementary nature of multi-omics data can provide valuable insights into the intricate molecular mechanisms underlying diseases. However, challenges such as limited sample size, high data dimensionality and differences in omics modalities pose significant obstacles to fully harnessing the potential of these data. The prior knowledge such as gene regulatory network and pathway information harbors useful gene–gene interaction and gene functional module information. To effectively integrate multi-omics data and make full use of the prior knowledge, here, we propose a Multilevel-graph neural network (GNN): a hierarchically designed deep learning algorithm that sequentially leverages multi-omics data, gene regulatory networks and pathway information to extract features and enhance accuracy in predicting survival risk. Our method achieved better accuracy compared with existing methods. Furthermore, key factors nonlinearly associated with the tumor pathogenesis are prioritized by employing two interpretation algorithms (i.e. GNN-Explainer and IGscore) for neural networks, at gene and pathway level, respectively. The top genes and pathways exhibit strong associations with disease in survival analyses, many of which such as SEC61G and CYP27B1 are previously reported in the literature.

Keywords: graph neural network; multi-omics; pathway; risk classification; interpretability

INTRODUCTION

To achieve a comprehensive and multidimensional understanding of complex and systemic diseases such as cancer, it is crucial to integrate multiple types of omics data [1–3], as analyzing a single omics offers only a partial understanding. While omics data can reveal various aspects of the human genome and enhance our understanding of cancer biology, the limited sample size available poses a significant challenge for the application of machine learning and deep learning techniques.

In recent years, deep learning tools have become increasingly prominent in oncology. Deep learning models have been extensively used for various tasks, including survival prediction [4–6], regulatory process analysis [7, 8], cancer classification [9–11], unveiling molecular mechanisms [12], identifying drug–target interactions [13] and yielding remarkable results. However, the high cost of acquiring multi-omics data for each patient often results in specific cancer-related multi-omics datasets having relatively small sample sizes. This can lead to overfitting and the curse of dimensionality when applying machine learning and deep learning methods to multi-omics data. Additionally, multi-omics data itself are plagued by issues such as high noise levels,

high missing rates and batch effects that severely impede the accuracy of model predictions. To effectively address these issues, numerous existing methodologies incorporate prior knowledge and network knowledge into their frameworks to alleviate the difficulty of model training while enhancing both generalization capabilities and interpretability [14].

Pathway information and regulatory network information are the most commonly used prior knowledge in recent studies. Gene pathways can integrate molecular information, covering physiological processes such as metabolism, cellular processes and human diseases, making them widely employed in omics data analysis. Pathway information can be obtained from the extensively used KEGG database [15], which provides gene pathway details and functional annotations. Many methods leverage gene pathways to guide network structure design or feature extraction algorithms. Elmarakeby *et al.* [16] developed a fully interpretable network that sequentially extracts gene, pathway and biological process features to predict disease states. DeepOmix [4] aggregates multi-omics data based on pathways and uses fully connected layers for prediction. PathCNN [17] compresses multi-omics data based on gene pathways using PCA. The compressed multi-omics features are then combined into an omics image that

Hongxi Yan is a phd candidate student at Beihang University.

Dawei Weng is a lecturer at Capital Medical University.

Dongguo Li is an associate professor at Capital Medical University.

Yu Gu is a professor at Capital Medical University.

Wenji Ma is a professor at Shanghai Jiao Tong University School of Medicine.

Qingjie Liu is an associate professor at Beihang University.

Received: January 19, 2024. Revised: March 11, 2024. Accepted: April 6, 2024

© The Author(s) 2024. Published by Oxford University Press.

This is an Open Access article distributed under the terms of the Creative Commons Attribution License (<https://creativecommons.org/licenses/by/4.0/>), which permits unrestricted reuse, distribution, and reproduction in any medium, provided the original work is properly cited.

is subsequently fed into a Convolution Neural Network for risk prediction. This method employs Grad-CAM [18] to explain the prediction results and identify differential pathways for long-term and non-long-term survival patients. However, these methods often rely solely on pathway information and use simple linear aggregation to combine omics data into pathway information, limiting their ability to provide comprehensive insights. Incorporating a regulatory network can supplement more detailed information for the neural network, enhancing its effectiveness.

The previous approaches [19, 20] to studying biological processes are based on molecular interaction networks between individual biological molecules, where nodes represent biological molecules, and edges describe the interactions between pairs of nodes. Multiple types of biological interaction networks representing different biological mechanisms [21] exist, based on various types of interactions such as protein–protein interaction networks [22] and gene regulatory networks [23]. Graph neural networks (GNNs) are commonly used for analyzing graph data in cancer research, where interaction networks provide supplementary prior knowledge. GNNs have been employed for tasks such as inferring regulatory networks [24], metastatic classification [25], cancer type classification [26], key gene prediction [27] and survival prediction [28–30]. However, few works have considered how to better utilize regulatory network knowledge across multiple omics datasets. The multilevel GNN employs a guidance graph that encompasses inter-omics and intra-omics regulatory relationships, thereby facilitating a more effective adaptation to multiomics data.

In this study, a new approach has been proposed to predict the risk of survival of patients. We propose a hierarchical deep learning model approach that comprises three components: a gene encoding graph neural network, a pathway aggregation block and a prediction module, corresponding to the extraction of gene information, pathway information and patient risk information, respectively. First, construct a guidance graph to establish regulatory relationships between genes and connections between different omics datasets. Gene encoding graph neural network generates gene-level features through a graph neural network guided by a guidance graph. Based on pathway information, the gene-level features are aggregated into pathway-level features in the pathway aggregation block through a Principal Component Analysis (PCA) initialized learnable layer, and further feature extraction is performed through a few hidden layer. The prediction module utilizes high-level pathway-level features to predict patient risk with pooling and fully connected (FC) layers. The multilevel graph neural network conducts further compression and extraction of features across various levels. At the gene level, it utilizes mutual information to filter out features of limited informational value, reducing superfluous data. Moreover, it leverages regulatory networks to explicitly guide the neural network in extracting intra-omics and inter-omics information, structurally avoiding the fusion of irrelevant gene information, thus enhancing the quality of gene-level features. At the pathway level, the multilevel graph neural network employs gene pathway information to further compress and extract gene features that collaboratively fulfill biological functions, reducing redundant information and increasing feature discrimination. Through such multi-level information extraction and compression, the multilevel graph neural network is able to unearth more valuable insights, consequently achieving superior performance on small datasets. The multi-level design of the model also bring improved interpretability, allowing for analysis of key factors from multiple dimensions. The study uses a node-mask-based explanation method to identify crucial genes and the Integrated Gradients

method [31] to identify critical gene pathways. Many of these crucial genes and pathways have been confirmed in past studies. Survival analysis of the identified crucial genes and pathways was conducted. These crucial genes and pathways have a strong correlation with patient risk, demonstrating the significance of the model's explanation methods.

METHOD

Overview

Our method takes in mRNA expression, copy number variation (CNV), DNA methylation profiling data and age as inputs, and outputs a two-dimensional (2D) vector that denotes the probabilities of low risk and high risk for each patient. For preprocessing of the data, given the low information density inherent in the omics data, mutual information on the training set was employed for gene selection for each omic data set separately. The overall framework of multilevel GNN is illustrated in Figure 1. The multilevel GNN comprises three components: a gene-encoding graph neural network that leverages both gene regulatory network and multi-omics data, aiming to enrich gene-level features with information on gene interactions based on specific regulatory relationships; a pathway aggregation block that aggregates genes within a pathway with a learnable linear layer to generate pathway-level features; and a prediction module that generates the prediction results, i.e. the probability of high and low risk of mortality, respectively. To facilitate the model with the ability of result interpretation, a mask-based neural network explanation method is employed to extract key genes that provide insights into the risk prediction. The overall structure of the key gene interpretation method is shown Figure 2. Specifically, this method utilizes gradient descent to adjust node-wise masks to minimize the conditional entropy between the output and ground truth, and the final node mask values represent the importance of the nodes. These pivotal genes are important for predicting the prognosis of patients. In addition, key pathways are identified using IGscore recognition. The IGscore, representing feature attributions, is calculated using the Integrated Gradients method, which integrates the gradients of a model's output with respect to pathway features along a path from a baseline to the actual pathway features.

Data preprocessing

When dealing with practical problems involving higher dimensional data, it is crucial to have a substantial amount of data for fitting in order to avoid the curse of dimensionality. Predicting gene-disease risk becomes particularly challenging due to the small number of patients for each cancer type, coupled with the high dimensionality of the genetic data. To tackle this challenge, mutual information was utilized to filter the multi-omics features. The K-nearest neighbors algorithm [32] was employed to calculate mutual information for the three omics datasets. As gene expression and methylation data are continuous, the formula for calculating mutual information is as follows:

$$MI(x) = \psi(N) - \langle \psi(N_x) \rangle + \psi(k) - \langle \psi(m) \rangle, \quad (1)$$

where $\psi(\cdot)$ denotes the digamma function, $\langle \cdot \rangle$ denotes the average function. N_x represents the total number of data points that belong to the same class as x and m represents the total number of data points within the neighborhood.

In each cross-validation iteration, we calculated the mutual information between all omics data and labels based on the training set. Data with mutual information greater than the mean mutual information were retained for training.

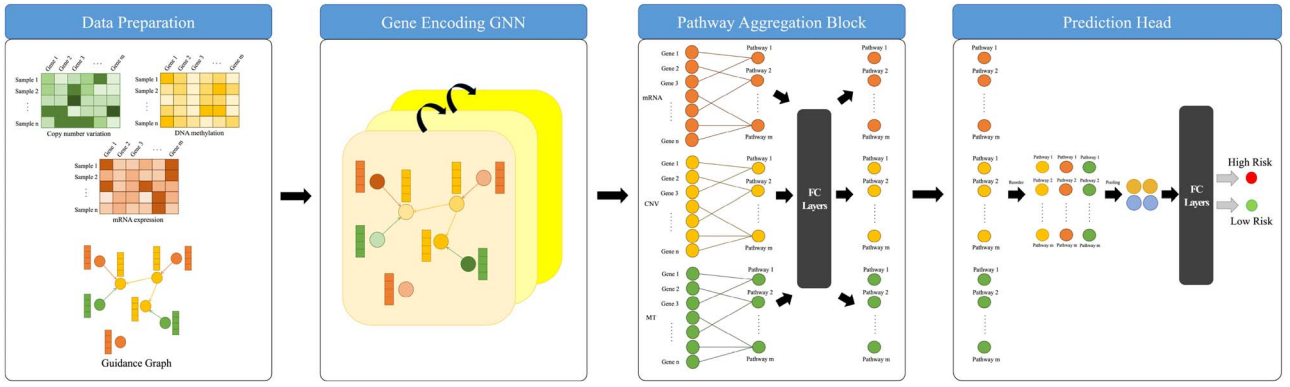


Figure 1. The algorithm comprises three modules: the graph neural network utilizes a guidance graph to encode features at the gene level, the pathway aggregation block aggregates gene features into pathway features based on pathway information and, finally, the prediction module uses pooling, FC layers to predict the risk.

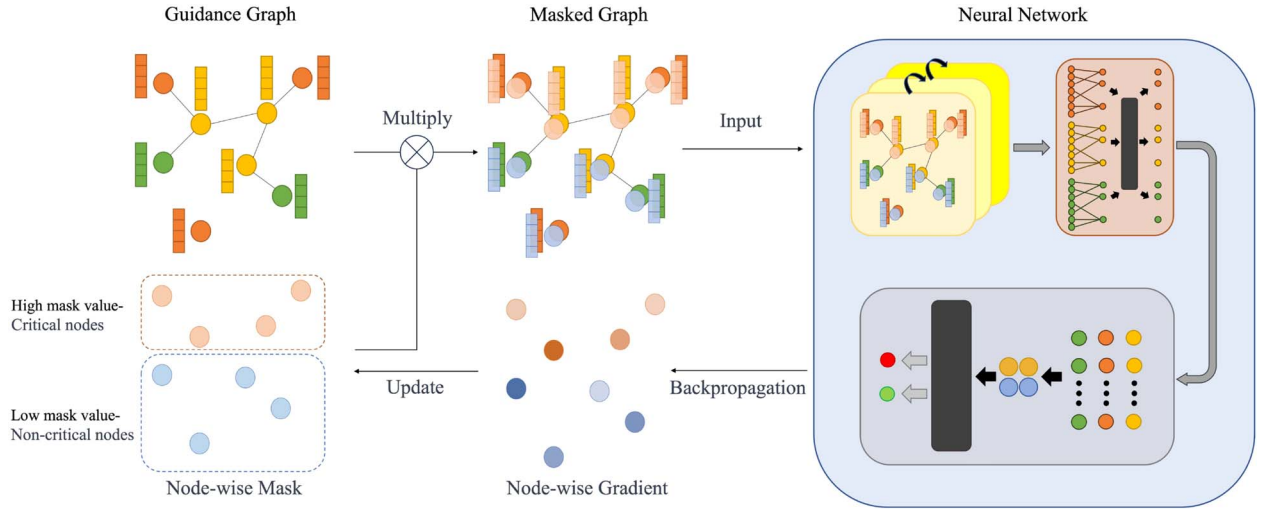


Figure 2. The gene interpretation algorithm assigns a mask to each node. The masked graph is obtained by multiplying the mask with the Guidance graph, and this masked graph is then input into the neural network. Through multiple iterations using gradient descent, the mask values are adjusted to minimize the error between the predicted result and the true value. In the end, critical nodes with high mask values and non-critical nodes with low mask values are obtained.

Guidance graph construction

To capture the connections between genes, as well as between different omics data for the same gene, we employed the same guidance graph $G = (V, E)$ as GLUE [7].

Firstly, for the mRNA data, a gene regulatory network $G_{mRNA} = (V_{mRNA}, E_{mRNA})$ using SCENIC [23] was constructed, where each edge e_{ij} represents a transcription factor (TF)-target pair from gene i to gene j . Since the SCENIC importance scores S_{ij} often have values greater than 1, the scores were normalized on all edges of each TF to the range of 0 to 1. These normalized scores are then used as the weights for the mRNA gene regulatory network, denoted as W_{mRNA} .

To link the data from different omics together, we created edges connecting CNV-mRNA (E_{CM}) and methylation-mRNA (E_{MM}) for the same gene. Since CNV often exhibits the same trend as gene expression, we constructed a positive edge ($w_{ij} = 1$) between CNV and mRNA. Furthermore, as methylation typically inhibits gene expression, we constructed a negative edge ($w_{ij} = -1$) between methylation and mRNA. The absolute values of edge weights between different omics were set to 1.

The nodes of the guidance graph consist of all nodes from each omics datasets, and the edges represent the union of edges connecting the mRNA regulatory network and different omics

datasets.

$$V = \{V_{mRNA}, V_{CNV}, V_{MT}\}$$

$$E = \{E_{mRNA}, E_{CM}, E_{MM}\}.$$

Multilevel GNN

Multilevel GNN consists of three parts: gene encoding graph neural network, pathway aggregation block and the prediction module. Figure 1 illustrates the overall algorithm.

Gene encoding GNN

Defining x_i as the expression value of the i th node. The gene encoding graph neural network initialize a random D -dimensional embedding e_i for each node. When a sample is fed into the neural network, the corresponding expression values are multiplied with the embeddings to obtain the input for the graph neural network $S = \{s_v = x_v \cdot e_v, \forall v \in V\}$.

The gene encoding graph neural network utilizes two layers of GraphSAGE [33] to encode the omics embeddings based on the guidance graph. GraphSAGE leveraging the guidance graph to aggregate node features as follows. Firstly, embeddings are

Algorithm 1 Gene Encoding Graph Neural Network**Input:**

\mathbf{G} : Guidance Graph;
 x_v : Omics Data;
 \mathbf{W}^k : Weight matrices;
 e_v : Node embedding;
 $\text{AGG}_k(\cdot)$: Differentiable aggregator functions;
 $N(\cdot)$: Neighborhood function;
 $\sigma(\cdot)$: non-linearity;
 $\text{Concat}(\cdot)$: Concatenation function;

Output: node embeddings $z_v, \forall v \in V$

```

1:  $h_v^0 \leftarrow x_v \cdot e_v, \forall v \in V$ 
2: for  $k \leftarrow 1$  to  $K$  do
3:   for  $v \in V$  do
4:      $h_{N(v)}^k \leftarrow \text{AGG}_k(\{h_u^{k-1}, \forall u \in N(v)\})$ 
5:      $h_v^k \leftarrow \sigma(\mathbf{W}^k \cdot \text{Concat}(h_v^{k-1}, h_{N(v)}^k))$ 
6:   end for
7: end for
8:  $z_v \leftarrow h_v^K, \forall v \in V$ 

```

collected from the neighboring nodes of each target node within the guidance graph. Subsequently, these neighbor features are combined using a learnable aggregation function. Finally, the aggregated features are transformed through a neural network layer, resulting in an updated representation of the node. This aggregation process utilizes gene interaction information based on specific regulatory relationships to enrich gene-level features. Algorithm 1 describes the embedding generation process when considering the entire guidance graph, $\mathbf{G} = (\mathbf{V}, \mathbf{E})$, and the expression values of all nodes X as input. We denote the output node embeddings as z_i for node i .

Pathway aggregation block

After obtaining the aggregated embedding of each gene, genes within the same pathway are aggregated to obtain pathway-level features in the pathway aggregation block. Specifically, the pathway aggregation block aggregates encodings $z_v, \forall v \in (\text{pathway}_i, \text{omic}_j)$ of nodes in the same omics within the same pathway using a learnable aggregation matrix \mathbf{W}_p^{ij} to obtain pathway-level features, denoted as PF. To better capture pathway-level features, two FC layers are further used to encode the pathway-level features PF, resulting in the final D -dimensional pathway features p_{ij} .

For each pathway on each omics, PCA can be used to reduce N gene features to M dimensions.

$$p_{ij}^{\text{origin}} = P_{ij} X_{ij}. \quad (2)$$

The matrix \mathbf{W}_p^{ij} is initialized using the compression matrix P_{ij} obtained from PCA. This initialization serves two purposes: firstly, PCA effectively compresses the features, and secondly, using a fixed initialization method improves training stability.

In addition, to maintain the independence of pathway features in each dimension, a cosine loss is applied to constrain the aggregation matrix. This constraint aims to maintain orthogonality

Algorithm 2 Pathway Aggregation Block**Input:**

X_v : Gene node features;
 Z_v : Node embeddings;
 \mathbf{W}_p^{ijm} : Pathway aggregation matrix;
 \mathbf{W}_{fc}^k : FC layer weight matrices;
 $\sigma(\cdot)$: non-linearity;
 $\text{Stack}(\cdot)$: Stack tensors function;

Output: pathway embeddings p_{ij}

```

1: for  $i \leftarrow 1$  to  $M$  do
2:   for  $j \in N$  do
3:      $\text{PF}_{ijm}^0 \leftarrow \mathbf{W}_p^{ijm} X_v \cdot Z_v$ 
4:   end for
5: end for
6: for  $k \leftarrow 1$  to  $K_i$  do
7:    $\text{PF}_{ijm}^k \leftarrow \sigma(\mathbf{W}_{fc}^k \cdot \text{PF}_{ijm}^{k-1})$ 
8: end for
9:  $p_{ij} \leftarrow \text{Stack}(\text{PF}_{ijm}^{K_i})$ 

```

across dimensions as much as possible.

$$L_{\text{ind}} = \sum_{mn} \cos(\mathbf{W}_p^{ijm}, \mathbf{W}_p^{ijn}). \quad (3)$$

To emphasize the impact of abnormal genes and highlight the influence of the original omics data, the gene encoding is multiplied once again by the input omics data before performing the aggregation. The specific aggregation formula is as follows:

$$\text{PF}_{ijm} = \mathbf{W}_p^{ijm} X_v \cdot Z_v. \quad (4)$$

The algorithm procedure is shown in Algorithm 2.

Prediction head

Lastly, a prediction module utilizes the pathway embeddings to predict the risk level of patients. Inspired by PathCNN, we performed sorting on the pathways before pooling. First, the pathway embeddings is arranged into a matrix $M_p \in R^{DNM}$, where N represents the number of pathways, M represents the number of multi-omic features and D represents the dimension of each multi-omic feature.

The pathways are organized in the order of their pairwise Pearson similarity scores after dimensionality reduction using PCA. First, the pairwise Pearson correlation is calculated between pathways by using the original PCA features p_{ij}^{origin} of each omics dataset for all samples within each pathway. The two pathways with the highest similarity score are placed at the first and second positions, followed by selecting the pathway with the highest similarity to the previous one in a sequential manner.

Due to the high dimensionality of pathway embeddings, using a FC layer directly for prediction poses significant challenges. Therefore, max pooling is applied to reduce the dimensionality

Table 1: Benchmark test results

| | Our | PathCNN [17] | Linear Regression | Neural Network | SVM | MiNet [34] |
|------|--------------------|--------------|-------------------|----------------|-------------|-------------|
| GBM | 0.772±0.006 | 0.755±0.009 | 0.668±0.039 | 0.692±0.030 | 0.685±0.037 | 0.690±0.032 |
| LGG | 0.885±0.006 | 0.877±0.007 | 0.816±0.036 | 0.791±0.031 | 0.884±0.017 | 0.854±0.027 |
| KIRC | 0.723±0.009 | 0.709±0.009 | 0.654±0.034 | 0.702±0.028 | 0.684±0.027 | 0.659±0.030 |

Note: The best results from each dataset are indicated in bold.

of reordered pathway embeddings. At last, two linear layers are utilized to predict the final outcome.

Gene explanation

We use a modified GNN-Explainer [35] to interpret the key genes. This demonstrates which genes are important in our prediction and, to some extent, also reflects which genes are important for the disease condition of patients.

The objective of GNN-Explainer is to select a subgraph that minimizes the conditional entropy H.

$$H(Y|G_S, X_S) = -\mathbb{E}[\log P_\Phi(Y|G = G_S, X = X_S)]. \quad (5)$$

Due to the lack of diversity in our graph among the samples and the relative sparsity of edges, we consider the nodes, which represent multiple omics datasets, as the primary target for explanation. Specifically, we constructed a mask matrix $M \in R^n$ for the nodes. The conditional entropy H can be optimized by adjusting the mask matrix M, $V \odot \sigma(M)$, where $\sigma(M)$ is a node-wise continuous mask for the nodes V, σ is the sigmoid function that maps the mask matrix M to $[0, 1]^n$. Therefore, the optimization objective can be rewritten as follows:

$$\min_M -\mathbb{E}[\log P_\Phi(Y = y|G = (V \odot \sigma(M), E))]. \quad (6)$$

During the explaining process, the mask matrix M is optimized through gradient descent. In each iteration, the mask matrix M is optimized using the following loss function:

$$\begin{aligned} Loss_{exp} = & \alpha * \log(\hat{y}_n) \\ & + \beta * \|\sigma(M)\|_1 \\ & + \gamma * \sum_{ij} (\sigma(M)_{ij} \log(\sigma(M)_{ij}) \\ & + \gamma * \sum_{ij} (1 - \sigma(M)_{ij}) \log(1 - \sigma(M)_{ij})), \end{aligned} \quad (7)$$

where α , β and γ are three coefficients, n represents the sample belonging to class n , \hat{y}_n is the model's estimated value for the sample in class n and $\|\cdot\|_1$ represents the L1 norm. The first term minimizes the error between the predicted results and the labels. The second term reduces the number of retained nodes, keeping only a small number of important nodes. The third and fourth terms are entropy losses that encourage discrete node feature masks.

Ultimately, the value corresponding to each node in the $\sigma(M)$ matrix represents the importance of that node. We computed the average z-scored importance of each gene across all samples as the final gene importance score. This allows us to select the key genes based on their importance.

Pathway explanation

The Integrated Gradients method [31] is used to identify key gene pathways. We calculated the IGscore for each feature of each pathway separately using the following formula:

$$IG_i = (S_i - S'_i) \int_0^1 \frac{\partial f(S'_i + \alpha(S_i - S'_i))}{\partial S'_i} d\alpha. \quad (8)$$

Here, S_i represents the pathway features output from the compressed matrix and S'_i represents the baseline. The subscripts i , respectively, represent the indices of the i th feature. $f(\cdot)$ represents the neural network after the compression matrix. Since the features of each pathway are represented by multiple multidimensional features, we took the average of the absolute values of the IGscore for each feature as the IGscore of the pathway. We used the z-score of pathways as the importance scores.

RESULT

Datasets

We utilized multi-omics data from The Cancer Genome Atlas (TCGA) database [36] to evaluate our model's generalizability across three cancer types: Glioblastoma Multiforme (GBM), Lower Grade Glioma (LGG) and Kidney Renal Clear Cell Carcinoma (KIRC). For these cancers, we obtained CNV, mRNA and methylation data from TCGA as model inputs. Additionally, age, a significant factor influencing patient survival time, was included as input for GBM and LGG samples.

The regulatory network among mRNA in the guidance graph was constructed using SCENIC [23], which integrates expression data and TF motif information for more accurate inference of gene regulatory relationships. This network enhances the neural network's capacity to predict disease risk by providing a precise understanding of cellular functions and signal transduction.

Gene pathways, another important biological information, were utilized in our survival analysis models. We obtained 146 gene pathways from the KEGG database, excluding those specific to certain diseases. These pathways encompass 4989 genes, although not every gene has complete data for all three omics types in the TCGA dataset. Therefore, the actual number of genes used in each omics type is slightly less than 4989, with the specific genes utilized listed in Table 1.

Considering the higher fatality rate of GBM, patients with a survival time exceeding 2 years were classified as long-term survivors (LTSS), while those with a survival time less than 2 years were classified as non-LTSS. For LGG and KIRC, which have lower fatality rates compared with GBM, patients with a survival time exceeding 3 years were considered LTSS, while those with a survival time less than 3 years were considered non-LTSS. The LTS and non-LTS groups had 55 and 234 cases for GBM, 156 and 75 cases for LGG and 154 and 69 cases for KIRC, respectively.

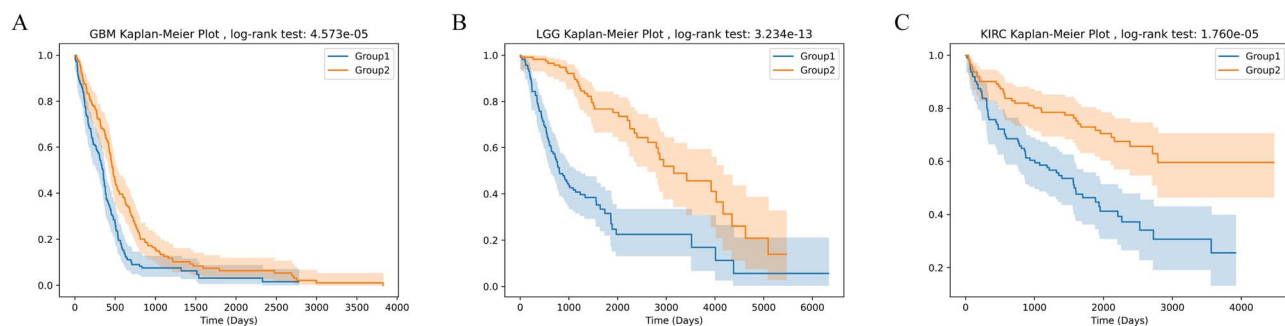


Figure 3. The patients were divided into high-risk and low-risk groups based on the predicted median, and there was a significant difference between the two groups in Kaplan-Meier analysis.

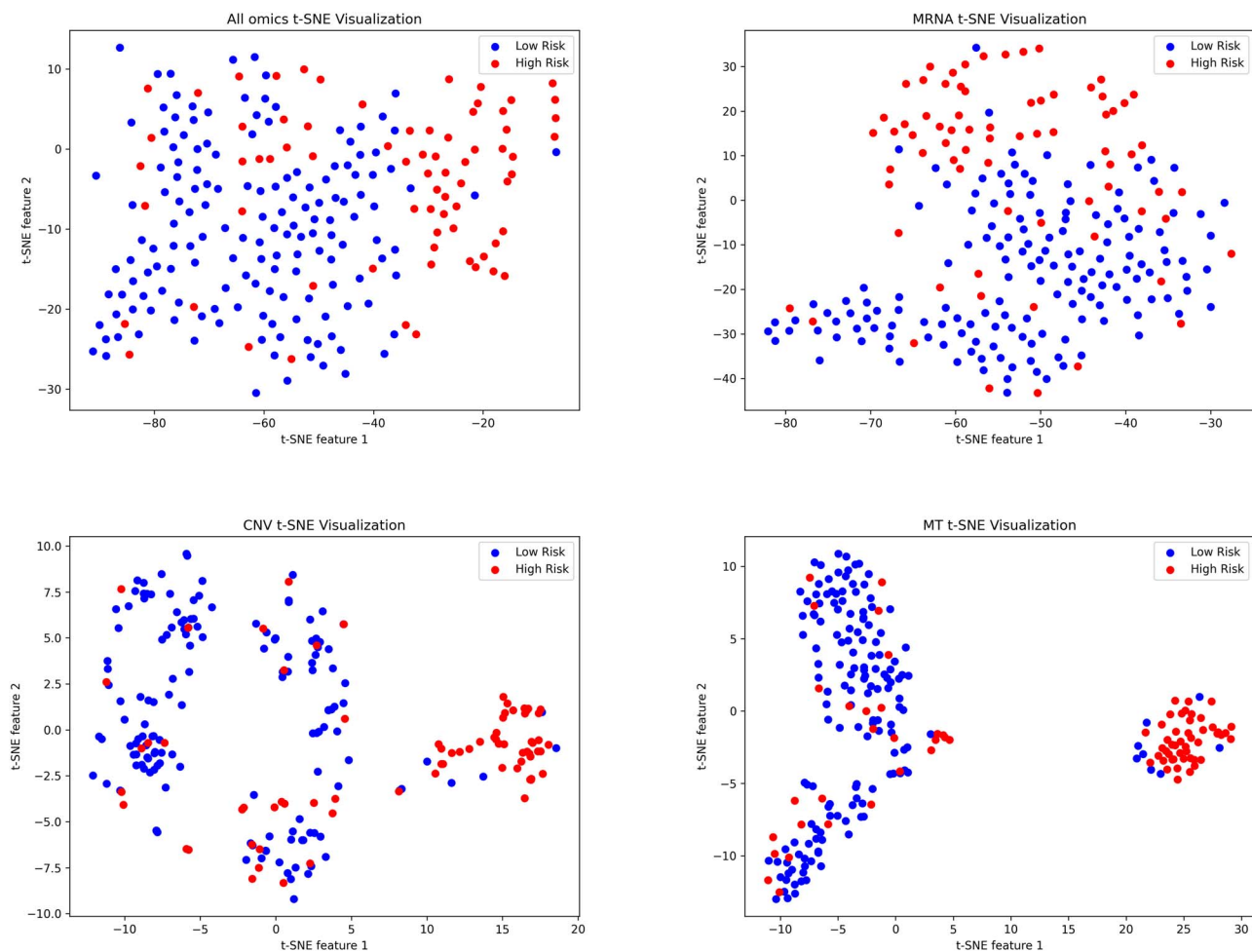


Figure 4. t-SNE was used to visualize the features of pathways trained on the LGG model. It can be observed that in all three omics and overall, there is a clear distinction in pathway features between high-risk and low-risk patients.

Feature validity analysis and visualization

Using the LGG dataset as an example, we initially conducted tests on this dataset. Based on the model's output, patients were classified into two subtypes: high-risk and low-risk. The Kaplan-Meier curve visualized a significant difference in survival time between these two subgroups (Figure 3). Subsequently, pathway-level features were separately visualized for each omics and overall using t-SNE (Figure 4). t-SNE effectively compressed the features into a 2D space, revealing distinct separability of samples from the two subtypes based on pathway-level features. This implies that by employing graph neural networks and pathway aggregation, discriminative pathway features can be extracted,

thereby enabling subsequent neural networks to more effectively predict patient risk.

Benchmark comparison

We compared our approach with two state-of-the-art models, PathCNN [17] and MiNet [34], as well as three classical methods, Linear Regression, Neural Network and Support Vector Machine (SVM), across four cancer datasets. We conducted 30 experiments using 5-fold cross-validation on each dataset, without a specifically partitioned test set. Similar to PathCNN, we combined all test sets from the 5-fold cross-validation, which encompasses the entire dataset, to calculate the Area Under Curve (AUC). The

Table 2: The results of different omics combinations

| | MRNA | MRNA&CNV | MRNA&MT | MRNA&CNV&MT |
|------|--------------|--------------|--------------|--------------|
| GBM | 0.752±0.0122 | 0.765±0.0070 | 0.765±0.0059 | 0.772±0.0060 |
| LGG | 0.847±0.0156 | 0.871±0.0078 | 0.868±0.0064 | 0.885±0.0064 |
| KIRC | 0.710±0.0118 | 0.720±0.0085 | 0.708±0.0080 | 0.723±0.0091 |

evaluation metric used in each experiment was the AUC of the entire dataset. The average AUC from the 30 experiments served as a comparative measure to assess the performance of each model. Table 2 presents the experimental results for all models on each dataset, demonstrating that our approach achieved superior AUC values compared with other methods across all three cancer datasets.

Ablation study

This section presents some ablation experiments for this study. First, we conducted ablation experiments on the main method using the LGG dataset (Table 3). To evaluate the effectiveness of pathway aggregation, we used a Neural Network as the baseline for comparison. We then experimented with a network that only contains the pathway aggregation module and the prediction head. This network achieves better AUC and stability compared with neural networks without pathway aggregation. By comparing the results of using a linear layer and a graph neural network before the aggregation module, it is evident that the graph neural network module can further enhance performance. In addition, to demonstrate the superior capability of the aggregation module, we replaced it with other dimensionality reduction methods for comparison. Since our dimensionality reduction module is used in neural networks, we selected two of the most commonly used dimensionality reduction modules in neural networks: max pooling and average pooling. For traditional dimensionality reduction methods, we chose an unsupervised dimensionality reduction method, PCA, for comparison. The results are presented in Table 4. As can be seen from the table, our method exhibits better performance. Although the 2/3-year division is the main division method in previous research [17, 37], we attempted experiments with different time divisions, and the results are shown in Supplementary Table 1 (see Supplementary Data available online at <http://bib.oxfordjournals.org/>). Finally, we attempted to use other clinical information in the model, and the results are presented in Supplementary Table 3 (see Supplementary Data available online at <http://bib.oxfordjournals.org/>). The results show that our method can achieve better results under most time divisions and other clinical data.

Multi-omics data improve model performance

To demonstrate the model's enhanced performance using multi-omics data and identify comparatively important omics, we conducted tests with different combinations of omics. Since mRNA data serve as a central bridge in the model, it was retained in all combinations. In two-omics combinations, edges between mRNA nodes in the guidance graph and between the two omics were preserved. Combinations having been tested separately include only mRNA, mRNA and CNV, and mRNA and MT, as illustrated in Table 5.

From the table, it can be observed that using only mRNA data gets the worst performance. The performance is similar

Table 3: Method ablation experiments

| Pathway Aggregation | Linear | GNN | AUC |
|---------------------|--------|-----|-------------|
| ✓ | | | 0.791±0.031 |
| ✓ | | | 0.836±0.009 |
| ✓ | ✓ | | 0.879±0.006 |
| ✓ | | ✓ | 0.885±0.006 |

Table 4: Ablation study for reduction methods

| | Our | MaxPooling | AvgPooling | PCA |
|------|-------------|-------------|-------------|-------------|
| GBM | 0.772±0.006 | 0.723±0.013 | 0.713±0.005 | 0.733±0.006 |
| LGG | 0.885±0.006 | 0.811±0.017 | 0.855±0.011 | 0.830±0.014 |
| KIRC | 0.723±0.009 | 0.609±0.014 | 0.634±0.022 | 0.670±0.022 |

Table 5: The gene explain results

| Gene | Omics | Importance Score | P-value | Adjusted P-value |
|---------|-------|------------------|-----------|------------------|
| Sec61g | mRNA | 17.39 | 1.567e-30 | 3.908e-27 |
| Cyp27b1 | mRNA | 16.72 | 2.638e-31 | 1.315e-27 |
| Cdk4 | mRNA | 8.311 | 2.074e-09 | 1.724e-07 |
| Ifna1 | CNV | 8.560 | 2.437e-13 | 5.066e-11 |
| Ifna6 | CNV | 8.308 | 3.156e-12 | 4.498e-10 |
| Ifna8 | CNV | 8.302 | 1.723e-13 | 4.093e-11 |
| Plcg1 | MT | 26.49 | 2.987e-04 | 0.01795 |
| Hexb | MT | 14.67 | 6.243e-04 | 0.03244 |
| Prkaca | MT | 12.51 | 9.378e-11 | 9.357e-08 |

Table 6: The number of genes included in each omics

| Cancer | mRNA | CNV | MT |
|--------|------|------|------|
| GBM | 3914 | 4876 | 3416 |
| LGG | 4631 | 4842 | 3675 |
| KIRC | 4633 | 4835 | 3920 |

when using two omics combinations, while it is best when utilizing data from all three omics simultaneously. This demonstrates that increasing the number of omics does improve the model's performance, highlighting each individual omic's importance. Furthermore, experiments using the combination of mRNA and CNV sometimes yield higher AUC means compared with those obtained with the combination of mRNA and MT. However, considering standard deviation values, results from combining mRNA and MT are more stable than those from combining mRNA and CNV. This suggests that, in survival prediction, CNV contains more potentially useful information than MT, but the model also finds it more challenging to effectively utilize the information from CNV.

Identification of key genes and pathways

We identified key genes using the GNN-Explainer-based interpretation method, and the results for LGG are shown in Table 6. The mean of the gene's importance scores across all samples is taken as the gene's overall importance score. For each omics, we selected the top three important key genes with adjusted P-values less than 0.05 for display. We divided patients into two groups, a high-importance-score group and a low-importance-score group, based on the mean importance score of a specific gene. Using this

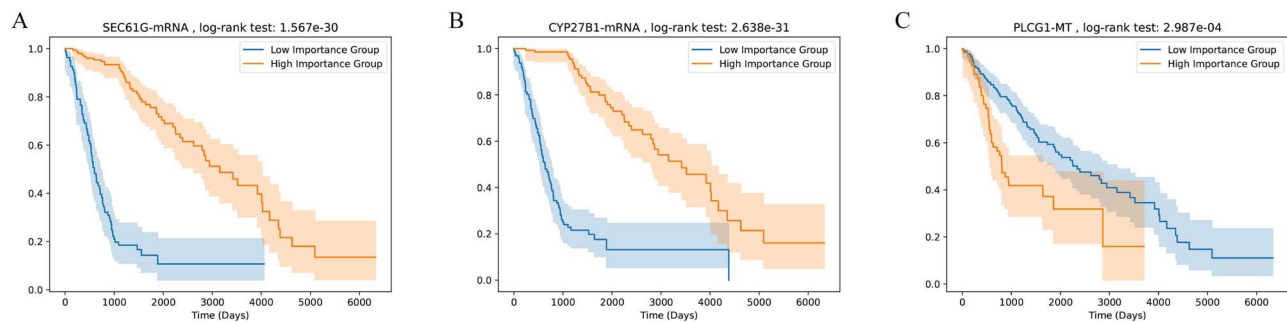


Figure 5. Kaplan–Meier curves for genes, dichotomized into two groups based on the median split of gene importance scores. The shaded area represents the 95% confidence interval.

grouping, we conducted survival analysis on the two groups of patients, as shown in Figure 5. In previous studies, these genes were also found to be associated with diseases. Zeng *et al.* [38] identified SEC61G as a pivotal regulator that promotes immune evasion and tumor growth in glioblastoma. Zhang *et al.* [39] found that CYP27B1 is overexpressed in LGGs, and its overexpression is associated with poor prognosis. Li *et al.* [40] found a significant correlation between the expression of PLCG1 and IDH1/2 status and patients’ clinical outcomes. Additionally, PLCG1-targeted drugs significantly inhibited tumor growth in IDH wild-type LGG cell lines and in mouse models.

We identified pathways with high importance scores in each omics using the Integrated Gradients method. The importance score for each pathway was determined by taking the median of all samples’ importance scores for that pathway. Pathways with z-score transformed importance scores greater than 1.96 were considered key pathways. In the LGG dataset, we identified a total of 19 key pathways, including 8 key pathways in mRNA omics, 4 key pathways in CNV omics and 7 key pathways in methylation omics. The importance score of a pathway reflects its impact on the prediction outcome. A higher score indicates a greater influence on the result. Therefore, we divided the samples into high and low score groups based on the median importance score of pathways and conducted survival analysis. Among the 19 pathways, 18 showed significant significance (P -value < 0.05) in survival analysis. Table 7 shows 18 pathways with significant correlation, along with their importance scores and P -values. Figure 6 displays the survival analysis for several pathways. MAPK has been identified as a key pathway in mRNA and MT omics. This is further supported by the survival analysis using importance scores, showing a strong correlation. Additionally, in previous studies, Nageswara *et al.* [41] identified the key regulatory factor of the MAPK signaling pathway in the occurrence of pediatric LGG tumors. Apart from this, other pathways have also been mentioned in previous studies. Jiang *et al.* [42] found that over-expressed crosstalk genes may be involved in the progression and poor prognosis of LGG through the ECM-receptor interaction pathway. Hirtz *et al.* [43] demonstrated the association between the expression levels of steroid biosynthesis enzymes and the survival risk of LGG patients.

Furthermore, we identified important pathways in GBM, and the results are presented in Supplementary Table 4 (see Supplementary Data available online at <http://bib.oxfordjournals.org/>). It can be seen that we identified some common pathways, such as Cytokine cytokine receptor interaction in mRNA omics and Neuroactive ligand receptor interaction in CNV omics. We also explained some pathways that have been validated in previous studies, such as the JAK-STAT signaling pathway [44] and Focal adhesion [45]. Experiments using different omics

Table 7: The pathway explain results

| Pathway | Omics | Importance Score | P-value |
|---|-------|------------------|-----------|
| Tgf beta signaling pathway | mRNA | 4.962 | 0.00142 |
| Steroid biosynthesis | mRNA | 3.774 | 0.0163 |
| MAPK signaling pathway | mRNA | 3.655 | 1.606e−11 |
| Ribosome | mRNA | 2.8 | 0.0153 |
| Glutathione metabolism | mRNA | 2.675 | 0.013 |
| Endocytosis | mRNA | 2.337 | 1.823e−06 |
| ErbB signaling pathway | mRNA | 2.26 | 7.447e−06 |
| Protein export | mRNA | 1.983 | 0.00133 |
| Cytosolic dna sensing pathway | CNV | 5.99 | 5.567e−08 |
| Cytokine cytokine receptor interaction | CNV | 4.654 | 2.614e−09 |
| Rig i like receptor signaling pathway | CNV | 4.085 | 5.544e−07 |
| Natural killer cell mediated cytotoxicity | CNV | 3.569 | 6.175e−12 |
| Regulation of actin cytoskeleton | MT | 4.609 | 4.019e−08 |
| Neuroactive ligand receptor interaction | MT | 4.026 | 3.977e−07 |
| MAPK signaling pathway | MT | 3.838 | 2.204e−07 |
| Endocytosis | MT | 3.601 | 8.831e−04 |
| Lysosome | MT | 3.405 | 9.078e−07 |
| ECM-receptor interaction | MT | 2.931 | 4.368e−07 |

have shown that methylation omics is important for our model. Therefore, compared with PathCNN, which did not identify any methylation omics, we identified four important pathways in methylation omics: Neuroactive ligand receptor interaction, Cytokine cytokine receptor interaction, Focal adhesion and Ubiquitin mediated proteolysis.

CONCLUSION

We have proposed a novel risk assessment algorithm, the multiomics-GNN, which effectively integrates multi-omics data, gene regulatory networks and pathway information to extract features and improve accuracy in predicting survival risk. Our model outperforms conventional methods when applied to diverse cancer datasets with multi-omics data. Moreover, we have demonstrated that our method based on multiple omics data achieves superior performance than on single omics data. Each additional omics contributes significantly and essentially to enhancing predictive performance, highlighting the effectiveness of the correlation-based multi-omics guidance

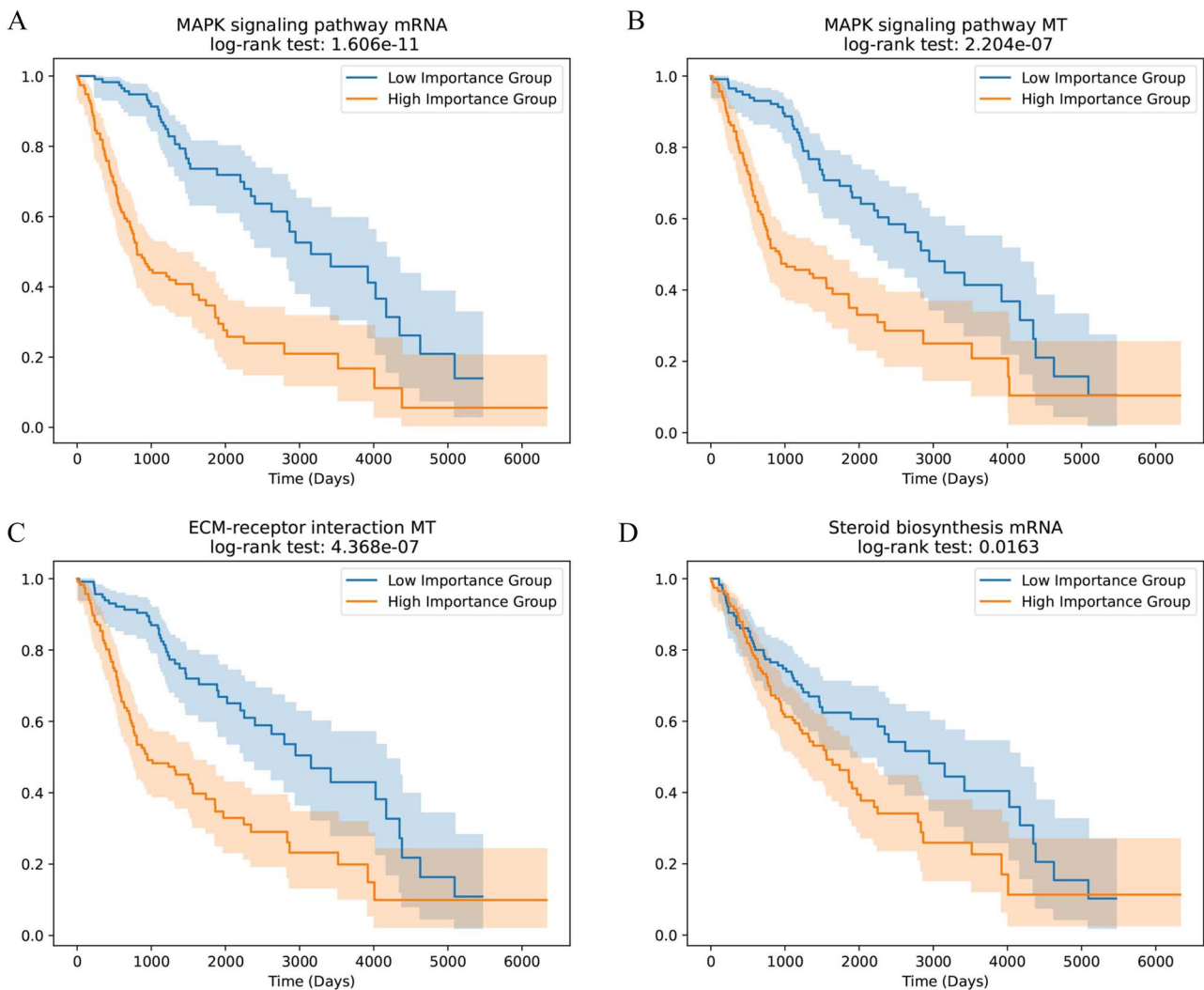


Figure 6. Kaplan-Meier curves for pathway, dichotomized into two groups based on the median split of pathway importance scores. The shaded area represents the 95% confidence interval.

graph we constructed. Furthermore, employing two interpretation methods at both the gene and pathway levels has revealed key factors that are strongly correlated with risk in survival analysis, and many of which have been corroborated by previous studies. In summary, this study showcases the potential of comprehensively and hierarchically incorporating multi-level information including multi-omics data, pathway information and gene regulatory information with graph neural network for accurate risk prediction while identifying nonlinear and risk-associated key factors. Moreover, graph neural networks demonstrate significant potential in processing multi-omics data and regulatory networks. Employing graph neural networks for handling and integrating data at various levels can enhance disease analysis, thereby facilitating the future integration of more omics data or the incorporation of MRI imaging data.

Key Points

- We proposed a Multilevel Graph Neural Network (Multilevel-GNN) algorithm, which hierarchically combines multi-omics data, gene regulatory networks and pathway information and improved the prediction performance compared with the existing methods.

- Multilevel-GNN constructed a guidance graph by explicitly establishing associations between and within omics data and employed a graph neural network to extract gene features that entail interactions between genes based on the guidance graph.
- Multilevel-GNN employed a learnable linear layer, which aggregates gene-level features into pathway-level features representing specific meaningful biological functions, thereby enhancing the model's accuracy as well as enabling interpretation at the pathway level.
- Multilevel-GNN employed two interpretation algorithms, GNN-Explainer and IGscore, to non-linearly identify key factors at the gene and pathway levels, enhancing the interpretability of neural network prediction decisions.

SUPPLEMENTARY DATA

Supplementary data are available online at <http://bib.oxfordjournals.org/>.

FUNDING

Science and Technology Innovation 2030 - Brain Science and Brain-inspired Artificial Intelligence Key Project (STI2030-Major Projects-2021ZD020400); National Key R&D Program of China (2022YFC3502500); Beijing Natural Science Foundation (L232103); National Natural Science Foundation of China (32100512); Young Elite Scientist Sponsorship Program by the China Association for Science and Technology (2020QNRC001); National Natural Science Foundation of China (61806010).

DATA AVAILABILITY

Our program is in <https://github.com/Y-Claw/Multilevel-GNN>. All the data comes from public databases, which can be obtained from public databases or from our GitHub projects.

REFERENCES

- Hasin Y, Seldin M, Lusis A. Multi-omics approaches to disease. *Genome Biol* 2017; **18**(1): 83.
- Hawkins RD, Hon GC, Ren B. Next-generation genomics: an integrative approach. *Nature Reviews Genetics* 2010; **11**(7): 476–48.
- Kristensen VN, Lingjærde OC, Russnes HG, et al. Principles and methods of integrative genomic analyses in cancer. *Nat Rev Cancer* 2014; **14**(5): 299–313.
- Zhao L, Dong Q, Luo C, et al. DeepOmix: a scalable and interpretable multi-omics deep learning framework and application in cancer survival analysis. *Comput Struct Biotechnol J* 2021; **19**: 2719–25.
- Sharifi-Noghabi H, Zolotareva O, Collins CC, Ester M. MOLI: multi-omics late integration with deep neural networks for drug response prediction. *Bioinformatics* 2019; **35**(14): i501–9.
- Hassanzadeh HR, Wang MD. An integrated deep network for cancer survival prediction using omics data. *Frontiers in Big Data* 2021; **4**: 568352.
- Cao ZJ, Gao G. Multi-omics integration and regulatory inference for unpaired single-cell data with a graph-linked unified embedding framework. *Nat Biotechnol* 2022; **40**: 1458–1466.
- Zhao M, He W, Tang J, et al. A hybrid deep learning framework for gene regulatory network inference from single-cell transcriptomic data. *Brief Bioinform* 2022; **23**: bbab568.
- Way GP, Greene CS. Extracting a biologically relevant latent space from cancer transcriptomes with variational autoencoders. *Pac Symp Biocomput* 2018; **80–91**: 2018.
- Jiao W, Atwal G, Polak P, et al. A deep learning system accurately classifies primary and metastatic cancers using passenger mutation patterns. *Nat Commun* 2020; **11**(1): 728.
- Liu J, Su R, Zhang J, Wei L. Classification and gene selection of triple-negative breast cancer subtype embedding gene connectivity matrix in deep neural network. *Brief Bioinform* 2021; **22**(5): bbaa395.
- Ma J, Yu MK, Fong S, et al. Using deep learning to model the hierarchical structure and function of a cell. *Nat Methods* 2018; **15**(4): 290–8.
- Zhao T, Hu Y, Valsdottir LR, et al. Identifying drug–target interactions based on graph convolutional network and deep neural network. *Brief Bioinform* 2021; **22**(2): 2141–50.
- Wysocka M, Wysocki O, Zufferey M, et al. A systematic review of biologically-informed deep learning models for cancer: fundamental trends for encoding and interpreting oncology data. *Bioinformatics* 2023; **24**(1): 1–31.
- Kanehisa M. The KEGG database. *Novartis Found Symp* 2002; **247**: 91–103.
- Elmarakeby HA, Hwang J, Arafeh R, et al. Biologically informed deep neural network for prostate cancer discovery. *Nature* 2021; **598**: 348–52.
- Oh JH, Choi W, Ko E, et al. PathCNN: interpretable convolutional neural networks for survival prediction and pathway analysis applied to glioblastoma. *Bioinformatics* 2021; **37**(Supplement_1): i443–50.
- Selvaraju RR, Cogswell M, Das A, et al. Grad-cam: visual explanations from deep networks via gradient-based localization. *Proc IEEE Int Conf Comput Vis* 2017; **37**(Supplement_1): 618–26.
- Barabási AL, Oltvai ZN. Network biology: understanding the cell's functional organization. *Nat Rev Genet* 2004; **5**(2): 101–13.
- McGillivray P, Clarke D, Meyerson W, et al. Network analysis as a grand unifier in biomedical data science. *Annu Rev Biomed Data Sci* 2018; **1**: 153–80.
- Vidal M, Cusick ME, Barabási AL. Interactome networks and human disease. *Cell* 2011; **144**(6): 986–98.
- Szklarczyk D, Gable AL, Lyon D, et al. STRING v11: protein–protein association networks with increased coverage, supporting functional discovery in genome-wide experimental datasets. *Nucleic Acids Res* 2019; **47**(D1): D607–13.
- Aibar S, González-Blas CB, Moerman T, et al. SCENIC: single-cell regulatory network inference and clustering. *Nat Methods* 2017; **14**(11): 1083–6.
- Li H, Sun Y, Hong H, et al. Inferring transcription factor regulatory networks from single-cell ATAC-seq data based on graph neural networks. *Nat Mach Intell* 2022; **4**(4): 389–400.
- Chereda H, Bleckmann A, Menck K, et al. Explaining decisions of graph convolutional neural networks: patient-specific molecular subnetworks responsible for metastasis prediction in breast cancer. *Genome Med* 2021; **13**: 1–16.
- Ramirez R, Chiu YC, Herrera A, et al. Classification of cancer types using graph convolutional neural networks. *Front Phys* 2020; **8**: 203.
- Schulte-Sasse R, Budach S, Hniss D, et al. Graph convolutional networks improve the prediction of cancer driver genes. In: *Artificial Neural Networks and Machine Learning–ICANN 2019: Workshop and Special Sessions: 28th International Conference on Artificial Neural Networks*, **11731**, 658–668, 2019. Munich, Germany, Springer Nature.
- Althubaiti S, Kulmanov M, Liu Y, et al. DeepMOCCA: a pan-cancer prognostic model identifies personalized prognostic markers through graph attention and multi-omics data integration. *bioRxiv preprint bioRxiv*: 2021.03.02.433454, 2021. <https://doi.org/10.1101/2021.03.02.433454>.
- Gao J, Lyu T, Xiong F, et al. MGNN: a multimodal graph neural network for predicting the survival of cancer patients. In: *Proceedings of the 43rd International ACM SIGIR Conference on Research and Development in Information Retrieval*, 1697–1700, 2020. New York, NY, United States, Association for Computing Machinery.
- Ramirez R, Chiu YC, Zhang SY, et al. Prediction and interpretation of cancer survival using graph convolution neural networks. *Methods* 2021; **192**: 120–30.
- M. Sundararajan, A. Taly, Q. Yan. Axiomatic attribution for deep networks. In: *International Conference on Machine Learning*, **3319–3328**, 2017. Sydney, Australia, OpenReview.net.
- Ross BC. Mutual information between discrete and continuous data sets. *PLoS One* 2014; **9**(2): e87357.
- Hamilton W, Ying Z, Leskovec J. Inductive representation learning on large graphs. *Adv Neural Inf Process Syst* 2017; **30**: 1025–1035.

34. Hao J, Masum M, Oh JH, et al. Gene- and pathway-based deep neural network for multi-omics data integration to predict cancer survival outcomes. *ISBRA* 2019; **15**:113–24.
35. Ying Z, Bourgeois D, You J, et al. Gnnexplainer: generating explanations for graph neural networks. *Adv Neural Inf Process Syst* 2019; **32**:9240–51.
36. Tomczak K, Czerwińska P, Wiznerowicz M. Review the cancer genome atlas (TCGA): an immeasurable source of knowledge. *Contemp Oncol/Współczesna Onkologia* 2015; **1A**:68–77.
37. Liang B, Gong H, Lu L, Xu J. Risk stratification and pathway analysis based on graph neural network and interpretable algorithm. *BMC Bioinform* 2022; **23**(1): 394.
38. Zeng K, Zeng Y, Zhan H, et al. SEC61G assists EGFR-amplified glioblastoma to evade immune elimination. *Proc Natl Acad Sci* 2023; **120**(32): e2303400120.
39. Zhang G, Chen A, Fang J, et al. Construction of a novel molecular typing and scoring system for anoikis distinguishes between different prognostic risks and treatment responsiveness in low-grade glioma. *Front Immunol* 2023; **14**:1105210.
40. Li T, Yang Z, Li H, et al. Phospholipase C γ 1 (PLCG1) overexpression is associated with tumor growth and poor survival in IDH wild-type lower-grade gliomas in adult patients. *Lab Invest* 2022; **102**(2): 143–53.
41. Nageswara Rao AA, Packer RJ. Advances in the management of low-grade gliomas. *Curr Oncol Rep* 2014; **16**:1–8.
42. Jiang Y, He J, Guo Y, et al. Identification of genes related to low-grade glioma progression and prognosis based on integrated transcriptome analysis. *J Cell Biochem* 2020; **121**(5–6): 3099–111.
43. Hirtz A, Lebourdais N, Thomassin M, et al. Identification of gender- and subtype-specific gene expression associated with patient survival in low-grade and anaplastic glioma in connection with steroid signaling. *Cancer* 2022; **14**(17): 4114.
44. Ou A, Ott M, Fang D, Heimberger A. The role and therapeutic targeting of JAK/STAT signaling in glioblastoma. *Cancer* 2021; **13**(3): 437.
45. Alowaidi F, Hashimi SM, Alqurashi N, et al. Cripto-1 overexpression in U87 glioblastoma cells activates MAPK, focal adhesion and ErbB pathways. *Oncol Lett* 2019; **18**(3): 3399–406.